Energy and Buildings 68 (2014) 121–129

Contents lists available at ScienceDirect

Energy and Buildings

journal homepage: www.elsevier.com/locate/enbuild

Energy and exergy analyses of solar drying system of red seaweed

Ahmad Fudholi*, Kamaruzzaman Sopian, Mohd Yusof Othman, Mohd Hafidz Ruslan

Solar Energy Research Institute, Universiti Kebangsaan Malaysia, Universiti Kebangsaan Malaysia 43600 Bangi, Selangor, Malaysia

ARTICLE INFO

Article history:
Received 14 April 2013
Accepted 24 July 2013

Keywords:
Energy
Exergy
Solar drying
Drying models
Red seaweed

ABSTRACT

A solar drying system was designed, constructed and tested for drying of seaweed. Seaweed is a potential source of renewable energy, and it can be converted into energy such as biofuel oil, biodiesel and gas. Red seaweed was dried to the final moisture content of 10% from 90% w.b in 15 h. Drying kinetics of red seaweed were investigated and obtained. The nonlinear regression procedure was used to fit three different drying models. The Page's model clearly showed a better fit to the experimental data between Newton's model and Henderson and Pabis model. The Page's model was resulted in the highest value of R^2 and lowest values of *MBE* and *RMSE*. At average solar radiation of about 500 W/m^2 and air flow rate 0.05 kg/s, the collector, drying system and pick-up efficiencies were found about 35, 27 and 95%, respectively. This study was performed with energy analysis and exergy analyses of the solar drying process of red seaweed. The specific energy consumption (SEC) of 2.62 kWh/kg was obtained. Moreover, the exergy efficiency of solar drying ranged from 1% to 93%, with an average of 30%. The values of improvement potential were found to be in the range of 0.3 and 630 W, with an average of 247 W.

1. Introduction

An alternative energy resource such as solar energy is becoming increasingly attractive. It is a clean energy, which has the world's most abundant permanent source of energy. It has also the potential to meet a significant proportion of the world's energy needs. In Malaysia, solar drying system has been great potential to be used in drying purpose, which is relevant to the local climate, with received an amount of 4.21–5.56 kWh/m^2 daily solar radiation intensity. Solar drying system is one of the most attractive and promising applications of solar energy systems. Demand for products of agriculture and marine products is a high quality dry. Most agricultural commodities and marine products require drying process in an effort to finally get a quality product. Traditionally, all the agricultural crops were dried under the sun. Drying is one of an important post handling process of agricultural production. It can extend shelf life of the harvested products, improve quality, improve the bargaining position of the farmer to maintain relatively constant price of his products and reduces post harvest losses and lower transportation costs since most of the water is taken out of the product during the drying process. Direct sun drying requires a large open space area, and very much dependent on the availability of sunshine, susceptible to contamination with foreign materials such as dusts, letters and are exposed to birds, insect and rodents. Hence, most agricultural produce that is intended to be stored must be dried first. Otherwise insects and fungi, which thrive in moist conditions, render them unusable [1–3].

Recently, there have been many reports on the drying kinetics of agricultural fruits and vegetables [4–6]. Thin-layer drying models also have been widely used for analysis of drying of various marine products [7–9]. Although many mathematical models have proposed to describe the drying process, a limited number of reported studies on mathematical models and drying kinetics of marine product such as seaweed in the literature. Seaweed is widely used in fabrication of food and medical industries and industry manufacture at present. Seaweed is a potential source of renewable energy, and it can be converted into energy such as biofuel oil and gas [10,11]. Demirbas [10] reported seaweed can be used for the production of bio-oil, biodiesel, ethanol, methane and hydrogen. By using thermochemical processes, oil and gas can be produced, and by using biochemical processes, ethanol, biodiesel and bio-hydrogen can be produced [11]. Ge et al. [12] reported brown seaweed *Laminaria japonica* can be used for the production of alginate, iodine and mannitol. They reported that seaweed excellent prospect as a potential feedstock for the production of bioethanol. Seaweed as an energy resource to produce biogas has been studied [13]. Gupta et al. [14] studied the effect of different temperatures on the drying kinetics and the phytochemical constituents of edible Irish brown seaweed, *Himanthalia elongate*. Their study involved the modeling of the term of Fick's diffusion equation for estimation of the diffusion coefficients. They concluded that the drying kinetics of seaweed can be accurately predicted using Newton's model, logarithmic model, and Henderson and Pabis model.

* Corresponding author. Tel.: +60 132924765.
E-mail addresses: a.fudholi@gmail.com, fudholi.solarman@gmail.com (A. Fudholi).

0378-7788/$ – see front matter
http://dx.doi.org/10.1016/j.enbuild.2013.07.072

Nomenclature

A_c	collector area (m^2)
a	drying constant
C	specific heat of air ($J\,kg^{-1}\,{}^\circ C^{-1}$)
d	mass of dry materials
exp	exponential
H	relative humidity (%)
h_o	absolute humidity of air leaving the drying chamber (%)
h_i	absolute humidity of air entering the drying chamber (%)
h_{as}	absolute humidity of the air entering the dryer at the point of adiabatic saturation (%)
k	drying constant
L	latent heat of vaporization of water at exit air temperature ($J\,kg^{-1}$)
M	moisture content
M_e	equilibrium moisture content
M_o	initial moisture content
MBE	mean bias error
m	mass flow rate (kg/s)
N	number of observations
n	drying constant
S	solar radiation (W/m^2)
R^2	coefficient of determination
$RMSE$	root mean square error
T	temperature (°C)
t	drying time
v	volumetric airflow (m^3/s)
W	weight of water evaporated from the product
w	mass of wet materials
ρ	density of air (kg/m^3)
η	efficiency

Subscripts

c	chamber
f	fan
i	inlet
o	outlet
exp	experimental
pre	prediction

Fudholi et al. [15] reported the effects of drying air temperature and humidity on the drying kinetics of red seaweed. The drying kinetics of red seaweed was studied using solar drying system [16], whereas a hot air chamber was used to determine the drying kinetics of brown seaweed *Eucheuma cottonii* [17]. The present study was carried out to select the best mathematical model to illustrate the drying behavior of red seaweed using the solar drying system.

Thermodynamics plays an important role to perform the energy efficiency of the industrial processes. The energy used in a system or process is significant and therefore represents an often reducible element of process cost. It is possible to identify the operating conditions in which potential savings can be made using an exergy analysis. Exergy is defined as the maximum amount of work which can be produced by a stream of matter, heat or work as it comes to equilibrium with a reference environment. Also, exergy analysis is a useful method to establish strategies for the design and operation of many industrial processes where the optimal use of energy is considered an important issue. This information is effective in determining the plant and the operation cost, the energy conservation, the fuel versatility and the pollutant. In the recent years, exergy analysis has been widely used for the performance evaluation of thermal systems. In the drying process, the aim is to use the minimum amount of energy for maximum moisture removal of the desired final conditions of the products [18,19]. Several studies have been conducted on exergy analyses of food drying. However, detailed literature review of the present study has shown that there is no information on energy and exergy analyses of solar drying system for seaweed. In this previous study conducted on experimental of solar drying has not been investigated using energy and exergy analysis method. However, little data currently exist in the performance of solar drying for seaweed. Few are found information about the improvement potential of the solar drying system in literature to the best of the authors' knowledge. The main objective of this paper is energy and exergy analyses of solar drying system for red seaweed. Therefore, this paper, as different other studies, concentrates on the performance, drying model and exergy analyses of solar drying system for red seaweed.

2. Materials and methods

2.1. Material

The red seaweed used in this study was obtained from Kedah, Malaysia. The initial moisture content of red seaweed was determined by measuring its initial and final weight using the hot air chamber at 120 °C until constant weight was obtained [20]. The average initial moisture content of red seaweed was obtained to be 90.6% w.b.

2.2. Experimental apparatus

A solar drying system was installed at the Green Energy Technology Innovation Park, UKM Malaysia in 2010. The drier is classified as a forced convection indirect type. A schematic diagram of the experimental solar drying system is shown in Fig. 1. It consists of auxiliary heater, blower, drying chamber and double-pass solar collector.

The collector width and length were 1.2 m and 4.8 m, respectively. The solar collector array consists of 4 solar collectors is shown in Fig. 2. The upper channel depth is 3.5 cm, and the lower depth is 7 cm. The bottom and sides of the collector have been insulated with 2.5 cm thick fiberglass to minimize heat losses. The cross-section of double-pass solar collector with finned absorber is shown in Fig. 3. The collector consists of the glass cover, the insulated and the black painted aluminum absorber. The size of the collector is 1.2 m wide and 4.8 m long. In this type of collector, the air initially enters through the first channel formed by the glass covering the absorber plate and then through the second channel formed by the back plate and the finned absorber plate. The size of the chamber is 2.4 m in length, 1 m width and 0.6 m in height.

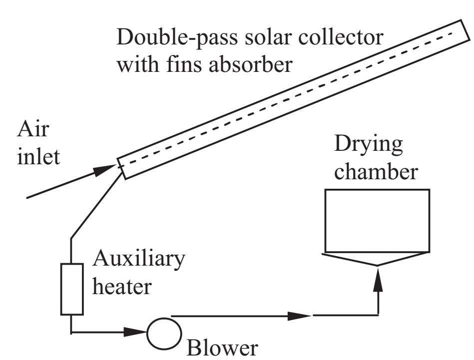

Fig. 1. Schematic diagram of solar drying system.

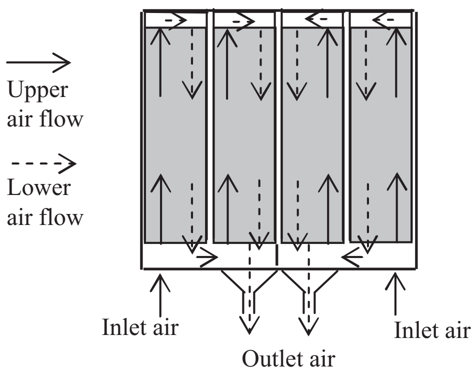

Fig. 2. The collectors of solar drying system.

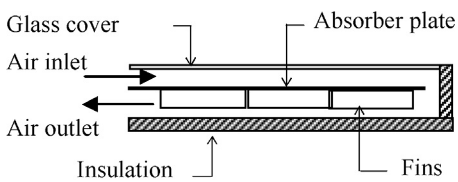

Fig. 3. The schematic of a double-pass solar collector with finned absorber.

2.3. Experimental procedure and uncertainties

An experiment was done between 08:00 and 18:00. During the drying experiments, the weather was sunny and no rain appeared. Broken seaweed was loaded over the trays of a drying chamber. The data were measured air temperature (ambient temperature, air temperature inlet and outlet of the collector), radiation intensity and air velocity, also measured the air temperature before it enters the dryer chamber, the temperature inside the dryer chamber, the temperature of the air out of the dryer chamber. Air temperature was measured by T-type thermocouple with an accuracy of 0.018 °C. Relative humidity sensors were installed in the inlet, middle, and outlet sections of the drying chamber. An air flow DTA 4000 anemometer to determine the air flow velocity in the solar collector was used. A LI-200 pyranometer with 1% accuracy was used. During the drying process, the temperature and relative humidity in the solar dryer were recorded at 1 min intervals during the experiments with the ADAM Data Acquisition System connected to a computer. Data were averaged for 30 min prior to analysis.

Drying experiment has been done for a large amount of red seaweed, 40 kg of red seaweeds was divided equally and then placed on 8 trays is shown in Fig. 4. To determine the moisture loss of drying red seaweed during experiments, seaweeds also were placed in the center of the drying chamber in a small tray. The moisture loss of red seaweed was determined by means of a Camry R9364 digital electronic balance having an accuracy of 0.01 g on top center of the dying chamber.

Table 1
Uncertainties during the measurements of the parameters.

Parameters	Unit	Uncertainty comment
Ambient air temperature	°C	±0.15
Collector inlet temperature	°C	±0.24
Collector outlet temperature	°C	±0.24
Chamber temperature	°C	±0.24
Solar intensity	W/m^2	±0.4
Air velocity	m/s	±0.2
Relative humidity	%	±0.16

Fig. 4. Photograph of seaweed in drying chamber.

During the measurements of the parameters, the uncertainties occurred were shown in Table 1. Uncertainty estimation is calculated by El-Sebaii et al. [21]:

$$X_R = [(x_1)^2 + (x_2)^2 + \ldots (x_n)^2]^{1/2} \quad (1)$$

where X_R = uncertainty in result; x_1, x_2,. . .x_n = uncertainty in the independent variables.

2.4. Mathematical modeling of drying curves

The moisture content was expressed as a percent wet basis. The experimental drying data for red seaweed were fitted to the thin layer drying models in Table 2, the moisture ratio (*MR*) can be calculated as [22]

$$MR = \frac{M - M_e}{M_0 - M_e} \quad (2)$$

where M_e = equilibrium moisture content; M_0 = initial moisture content.

The moisture content of materials (M) can be calculated by two methods on the basis of either wet or dry basis using the following equation.

The moisture content wet basis

$$M = \frac{w(t) - d}{w} \times 100\% \quad (3)$$

The moisture content dry basis

$$X = \frac{w(t) - d}{d} \quad (4)$$

where $w(t)$ = mass of wet materials at instant t; d = mass of dry materials.

The values of the coefficient of determination (R^2), mean bias error (*MBE*) and root mean square error (*RMSE*) were used to determine the quality of the drying model. The highest R^2 values and the

Table 2
Several models of drying.

No.	Model name	Model
1	Newton	MR = exp ($-kt$)
2	Page	MR = exp ($-kt^n$)
3	Henderson and Pabis	MR = a exp ($-kt$)

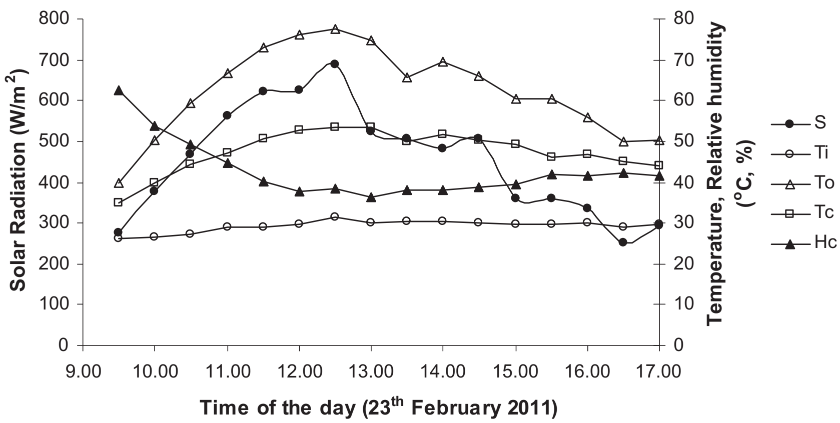

Fig. 5. Temperatures (inlet, outlet and chamber), relative humidity of chamber and solar radiation.

values of *MBE* and the lowest *RMSE* were selected to estimate the drying curve is the best [23,24].

$$MBE = \frac{1}{N}\sum_{i=1}^{N}(MR_{pre,i} - MR_{\exp,i})^2 \quad (5)$$

$$RMSE = \left[\frac{1}{N}\sum_{i=1}^{N}(MR_{pre,i} - MR_{\exp,i})^2\right]^{1/2} \quad (6)$$

2.5. Energy analysis

The specific energy consumption (SEC) of the solar drying system was obtained using Eq. (7), as reported by Fudholi et al. [25]

$$SEC = \frac{P_t}{W} \quad (7)$$

where *SEC* = specific energy consumption (kWh/kg); *W* = mass of water evaporated from the product (kg); P_t = total energy input to the dryer (kWh).

The mass of water removed (*W*) from a wet product can be calculated by:

$$W = \frac{m_o(M_i - M_f)}{100 - M_f} \quad (8)$$

where m_o = initial total crop mass (kg); M_i = initial moisture content fraction on wet basis; M_f = final moisture content fraction on wet basis.

The thermal efficiency of the solar collector was estimated by the following equation:

$$\eta_c = \frac{mC(T_o - T_i)}{A_c S} \times 100\% \quad (9)$$

where *m* = mass flow rate (kg/s); *C* = specific heat of air (J kg^{-1} °C^{-1}); A_c = collector area (m^2); T_i = inlet air temperature (°C); T_o = outlet air temperature (°C); *S* = solar radiation intensity (W/m^2).

System drying efficiency was defined as the ratio of the energy required to evaporate from the moisture to the heat supplied to the drier. The system efficiency for forced convection solar dryers need to take into account the energy consumed by fan/blower, can be calculated as [26]

$$\eta = \frac{WL}{SA_c + P_f} \quad (10)$$

where *W* = weight of water evaporated from the product (kg); *L* = latent heat of vaporization of water at an exit air temperature (J kg^{-1}).

Pick-up efficiency determines the efficiency of moisture removal of the drying air from the product, can be calculated as

$$\eta = \frac{h_0 - h_i}{h_{as} - h_i} = \frac{W}{\nu\rho t(h_{as} - h_i)} \quad (11)$$

where h_o = Absolute humidity of air leaving the drying chamber (%); h_i = Absolute humidity of air entering the drying chamber (%); h_{as} = Absolute humidity of the air entering the dryer at the point of adiabatic saturation (%); ν = volumetric air flow (m^3/s); ρ = density of air (kg/m^3); *t* = drying time (s).

2.6. Exergy analysis

The exergy values are calculated by using the characteristics of the working medium from a first-law energy balance. For this purpose, the general form of exergy equation applicable for a steady flow system may be expressed as [18]

$$Ex = \dot{m}_{da}C_{pda}\left[(T - T_a) - T_a \ln\frac{T}{T_a}\right] \quad (12)$$

For exergy inflow of drying chamber:

$$Ex_{dci} = \dot{m}_{da}C_{pda}\left[(T_{dci} - T_a) - T_a \ln\frac{T_{dci}}{T_a}\right] \quad (13)$$

For exergy outflow of drying chamber:

$$Ex_{dco} = \dot{m}_{da}C_{pda}\left[(T_{dco} - T_a) - T_a \ln\frac{T_{dco}}{T_a}\right] \quad (14)$$

However, during the solar drying process, the exergy losses are determined using Eq. (15):

$$Ex_{loss} = Ex_{dci} - Ex_{dco} \quad (15)$$

The exergy efficiency can be defined as the ratio of exergy use (investment) in the drying of the product to exergy of the drying air supplied to the system. However, it is explained as the ratio of exergy outflow to exergy inflow for drying chamber. Considering this definition, the exergy efficiencies of drying chamber can be determined. Thus, the general form of exergy efficiency is written as [18,19]

$$\eta_{Ex} = \frac{Ex_{dco}}{Ex_{dci}} = 1 - \frac{Ex_{loss}}{Ex_{dci}} \quad (16)$$

Van Gool [27] has proposed that maximum improvement in the exergy efficiency of a system or process is obviously achieved when the exergy loss (Ex_{loss}) is minimized. He suggested that it is useful to employ the concept of an exergy "improvement potential"

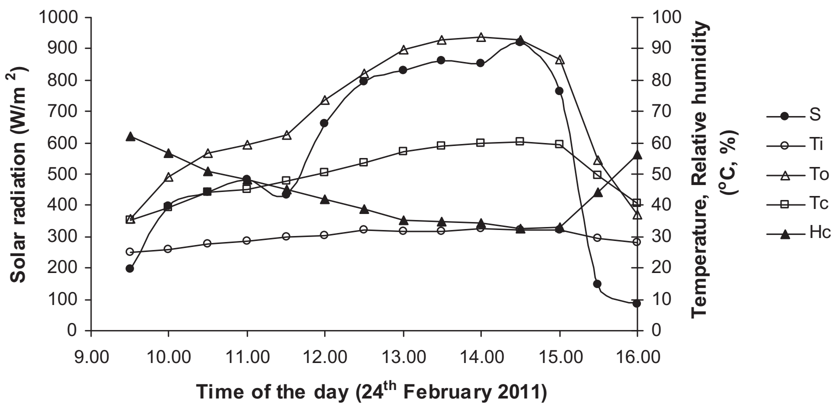

Fig. 6. Drying temperatures (inlet, outlet and chamber), relative humidity of chamber and solar radiation.

when analyzing different processes or sectors of the economy. The improvement potential (IP) of a system or process is given by

$$IP = (1 - \eta_{Ex})Ex_{loss} \quad (17)$$

3. Results and discussion

During the two days of experiments, the variations of the solar radiation (S), collector inlet air temperature (T_i), collector outlet air temperature (T_o), drying chamber air temperature (T_c) and average relative humidity of drying chamber (H_c) are shown in Figs. 5 and 6. From these figures, the daily mean of the drying chamber air temperature, relative humidity of drying chamber and solar radiation range from about 35–60 °C, 32–63%, 83–920 W/m^2, respectively. During the two days drying, the daily averages of relative humidity at the drying chamber were obtained 43 and 44%.

About 40 kg of red seaweed in the chamber, drying of seaweed takes two days to reduce the initial moisture content of 94.6–10%, equivalent to 40–4.44 kg. During the two days drying, the daily averages of air temperature at the drying chamber were 45 and 50 °C and average solar radiations 453 and 562 W/m^2 at a mass flow rate 0.0536 kg/s, as shown in Figs. 7 and 8. The efficiency of collector varies from 26% to 80%, and the average efficiency of the collector was about 35%, as shown in Figs. 7 and 8.

The kinetic curve of drying red seaweed at two conditions were decreased moisture content wet basis of drying time, as shown in Fig. 9. Drying curve can also show the profile change in moisture content (X) versus drying time (t), as shown in Fig. 10. The drying kinetics of seaweed can be accurately predicted using Newton's model, logarithmic model and Henderson–Pabis model Gupta et al. [14]. Azoubel et al. [28] reported that Page's model clearly improved the simulation in comparison with the results obtained using the diffusion model, having the best fit to the experimental data, with calculated average error ranging from 1.89% to 12.76% and R^2 values greater than 0.99. Page's model has shown a better fit than other models at accurately simulate the drying curves of chili pepper [24], rapeseed [29], green beans [30], okra [31], kiwi [32] among others.

Page's equation can also be written into the equation

$$\ln(-\ln MR) = \ln k + n \ln t \quad (18)$$

Eq. (9) is the relationship ln (−ln MR) versus t, was the curve of the logarithmic equation, as shown in Fig. 12. Henderson and Pabis equation can also be written by equation

$$\ln MR = -kt + \ln a \quad (19)$$

From Eq. (19), a plot of ln MR versus drying time gives a straight line with intercept = ln a, and slope = k. Graf MR versus ln t, as shown in Fig. 13, obtained the value k = 0.3327 and the value of a = 0.5367.

A set of experiments was conducted to develop a drying model to simulate the drying curves of red seaweed. Drying models were fitted to the experimental data of drying in the form of changes in moisture content versus drying time. In these drying models, changes in moisture content versus time calculated using Excel software. Fitting some of the drying model has been done with the experimental data, as shown in Figs. 11–13. The values of R^2, MBE, $RMSE$ and the parameters a, n and the constant k for the different models were listed in Table 3. The highest value of R^2 and lowest value of MBE and $RMSE$ indicated the goodness of the fit. Results presented in Table 3 showed that the Page's model has the highest value of R^2 (0.9676), as well as the lowest values of MBE (0.00023) and $RMSE$ (0.01510), compared to Newton's model and Henderson and Pabis model. Accordingly, the Page's model was selected as the suitable model to represent the thin layer drying

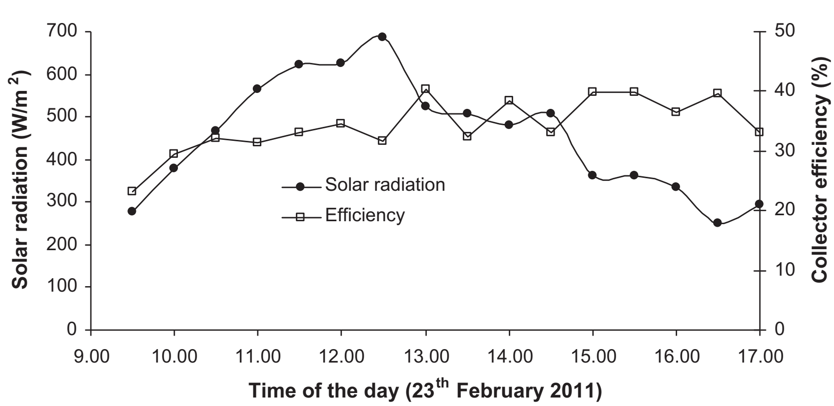

Fig. 7. Efficiency of collector and solar radiation at m = 0.0536 kg/s for the 1st drying day.

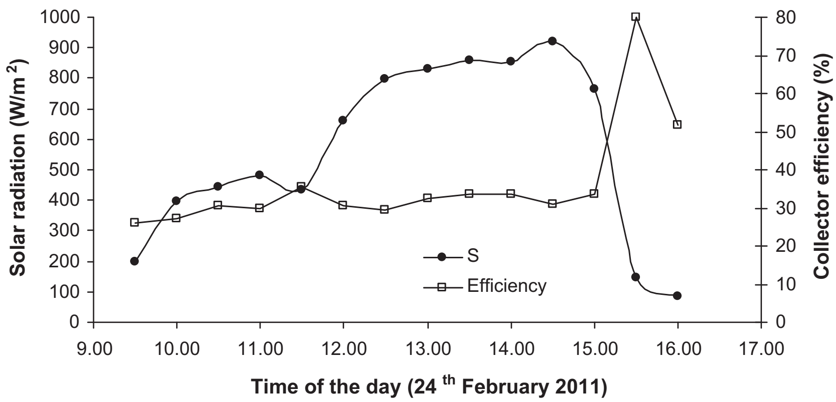

Fig. 8. Efficiency of collector and solar radiation at $m = 0.0536$ kg/s for the 2nd drying day.

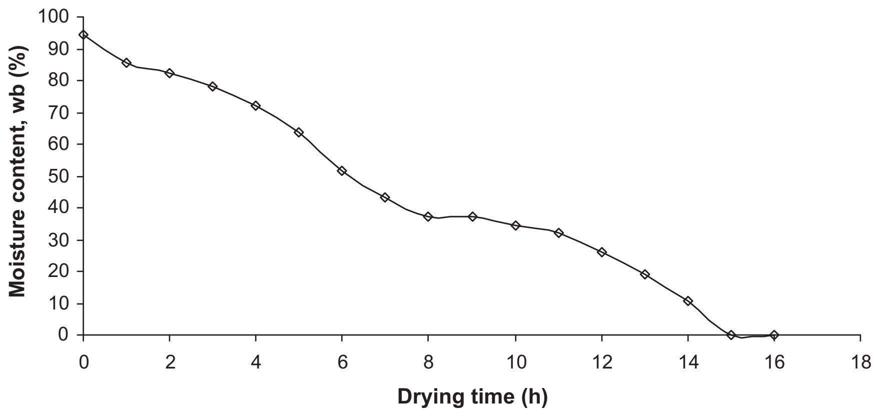

Fig. 9. Drying curve: wet basis moisture content versus drying time.

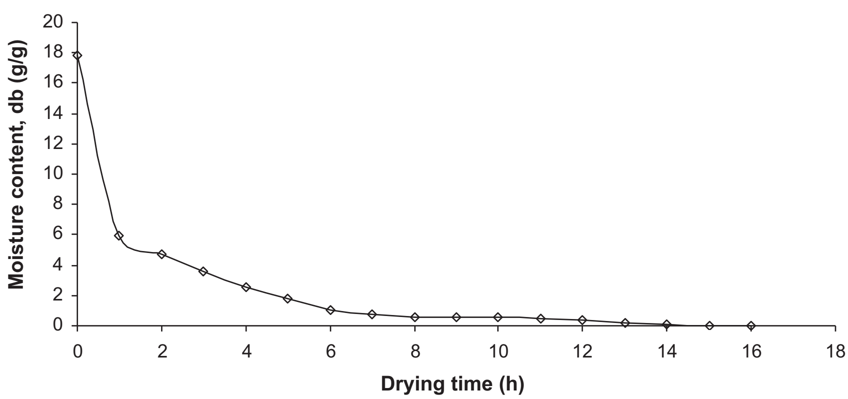

Fig. 10. Drying curve: dry basis moisture content versus drying time.

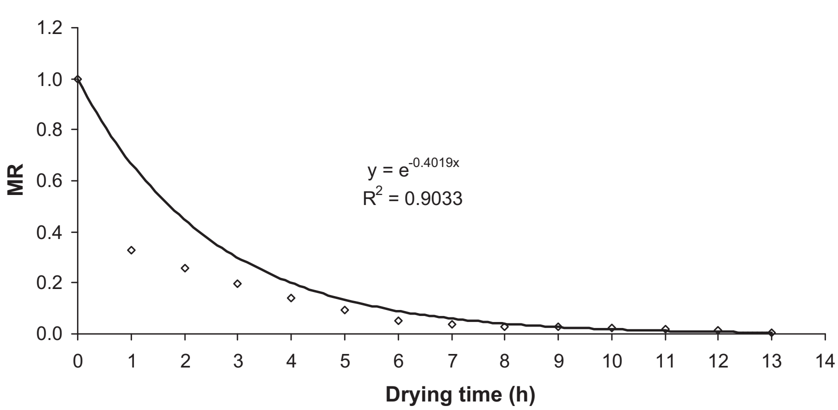

Fig. 11. Plot of *MR* versus drying time (Newton's model).

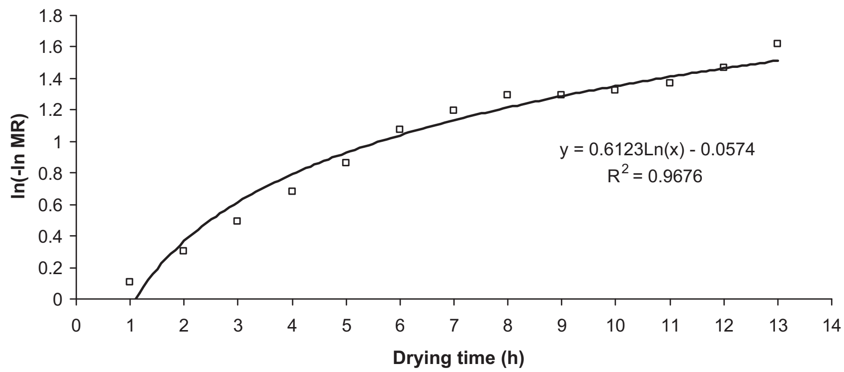

Fig. 12. Plot of ln (−ln *MR*) versus drying time (Page's model).

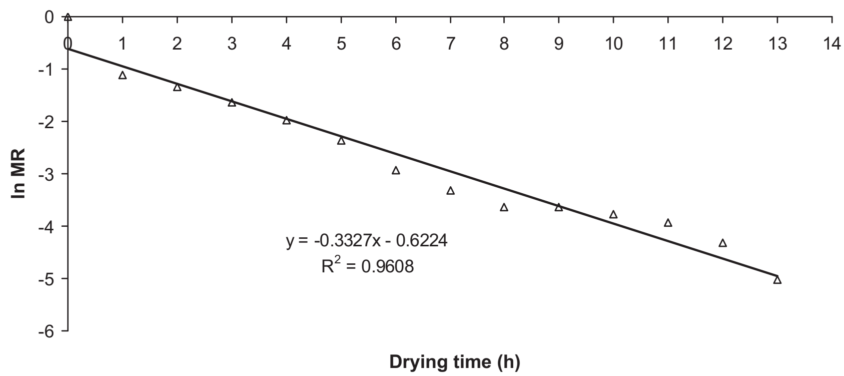

Fig. 13. Plot of ln *MR* versus drying time (Henderson and Pabis model).

Table 3
Constants value fitting of the drying models.

Model	*a*	*k*	*n*	R^2	*MBE*	*RMSE*
Newton		0.4019		0.9033	0.00529	0.07274
Page		0.9442	0.6123	0.9676	0.00023	0.01510
Henderson and Pabis	0.5367	0.3327		0.9608	0.00024	0.01539

behavior of red seaweed. This is in accordance with Fudholi et al. [15–17] that Page's model was shown to be a better fit to drying seaweed among other one-term exponential models thin layer drying models. On the other hand, as far as the drying behavior of lemon grass is concerned, the Newton's model showed a better fit to the experimental data among other semi-theoretical models [33]. Comparison of experimental MR with predicted MR from models drying. The distribution of experimental values in the vicinity of the straight line shows the expected value of Page's model, as shown in Fig. 14.

The experimental results showed that solar drying without auxiliary heating of 40 kg of dry red seaweed required about 10% water content within 15 h (2 days of drying) to yield 4.44 kg of dried red seaweed. A 2.62 kWh/kg was obtained for the specific energy consumption, was calculated using Eq. (7). However, the weight of water evaporated from the red seaweed obtained using Eq. (8) was

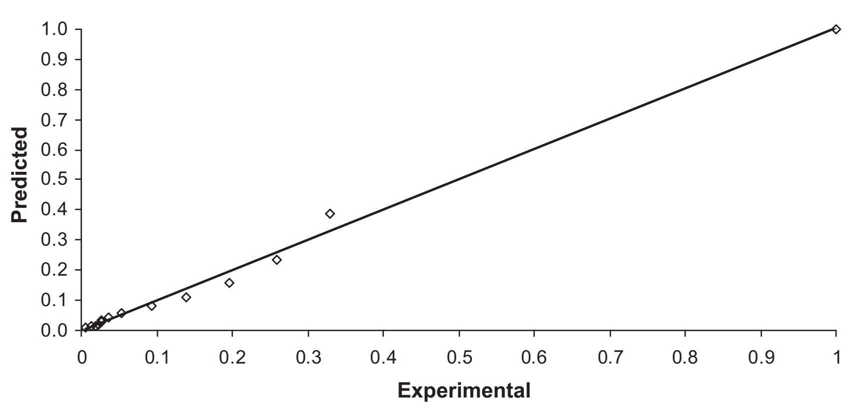

Fig. 14. Comparison of experimental MR with predicted MR of Page model.

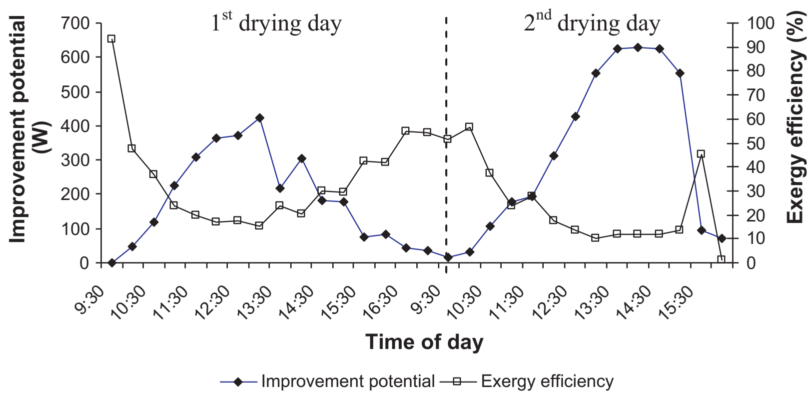

Fig. 15. The variation of improvement potential and exergy efficiency as a function of time.

Table 4
Saturated steam [34].

Temperature (°C)	Pressure (kPa)	Enthalpy (sat. vap.) (kJ/kg)	Latent heat (kJ/kg)	Specific volume (m^3/kg)
30	4.25	2556	2431	32.9
40	7.38	2574	2407	19.5
50	12.3	2592	2383	12.0
60	19.9	2610	2359	7.67
70	31.2	2627	2334	5.04

Table 5
Performance of solar drying for red seaweed.

Parameters	Unit	Value
Initial weight (total)	kg	40
Final weight (total)	kg	4.44
Initial moisture content (wet basis)	%	90
Final moisture content (wet basis)	%	10
Mass flow rate	kg/s	0.05
Average solar radiation	W/m^2	500
Average ambient temperature	°C	30
Average drying chamber temperature	°C	48.6
Average drying chamber humidity	%	43
Drying time	h	15
Blower energy	kWh	0.45
Specific energy consumption	kWh/kg	2.62
Overall heat collection (thermal) efficiency	%	35
Overall drying efficiency, up to 10% wet basis	%	27
Pick-up efficiency, up to 10% wet basis	%	95
Overall exergy efficiency, up to 10% wet basis	%	30
Overall improvement potential	kW	0.247

35.56 kg. Adding L = 2383 kJ/kg (662 Wh/kg) for T = 50 °C as shown in Table 4, t = 15 h, and S = 500 W/m^2 to Eq. (10) yielded a drying efficiency of 27.1%. By using Eq. (11) and a psychometric chart determined the pick-up efficiency to be 94.51%. During the solar drying process, the exergy efficiency was calculated by using Eq. (16), and it was in the range of 1–93% with an average of 30%, as shown in Fig. 15. By using Eq. (17), the values of improvement potential were found to be in the range of 0.3 and 630 W, with an average of 247 W as shown in Fig. 15. The summary of the experimental results and observations are given in Table 5.

4. Conclusion

A solar drying system was designed, constructed and tested for drying of seaweed. Kinetic curves of drying of seaweed known to use this system. The nonlinear regression procedure was used to fit three different drying models. The models were compared with experimental data of red seaweed drying at the daily average air temperature about 50 °C. The fit quality of the models was evaluated using the coefficient of determination (R^2), mean bias error (*MBE*) and root mean square error (*RMSE*). The highest values of R^2 (0.9676), the lowest *MBE* (0.00023) and *RMSE* (0.001510) indicated that the Page model is the best mathematical model to describe the drying behavior of red seaweed.

The solar collector, drying system and pick-up efficiency rates of about 28%, 13% and 45%, respectively, at the average solar radiation of about 500 W/m^2 and air flow rate of 0.05 kg/s. A maximum and minimum the collector efficiency about 80% and 23%, respectively, was observed, and the drying temperature varied between 35 °C and 60 °C, with an average of 48.6 °C. A 2.62 kWh/kg was obtained for the specific energy consumption. The values of exergy efficiency varied between 1% and 93%. The values of improvement potential were found to be in the range of 0.3 and 630 W, with an average of 247 W.

Acknowledgements

The authors would like to thank the Yayasan Felda for funding this research grant (RMK9 RS-DL-001-2007), and the Solar Energy Research Institute (SERI), Universiti Kebangsaan Malaysia for support.

References

[1] K. Sopian, M.Y. Othman, S.H. Zaidi, Advances in Solar Assisted Drying System for Marine and Agricultural Products, 2012, Available from: http://ases.conference-service.net/resources/252/2859/pdf/SOLAR 2012 (accessed April 2013).
[2] A. Fudholi, K. Sopian, M.H. Ruslan, M.A. Alghoul, M.Y. Sulaiman, Review of solar dryers for agricultural and marine products, Renewable and Sustainable Energy Reviews 14 (1) (2010) 1–30.
[3] M.H. Ruslan, A. Fudholi, M.Y. Othman, M.S.M. Azmi, A. Zaharim, K. Sopian, The double pass solar dryer for drying palm oil fronds, in: Proceedings of the 10th WSEAS International Conference on System Science and Simulation in Engineering (ICOSSSE'11), Penang, Malaysia, 2011, pp. 143–149.
[4] A.O. Dissa, D.J. Bathiebo, H. Desmorieux, O. Coulibaly, J. Koulidiati, Experimental characterization and modelling of thin layer direct solar drying of Amelie and Brooks mangoes, Energy 36 (5) (2011) 2517–2527.
[5] I. Doymaz, Effect of citric acid and blanching pre-treatments on drying and rehydration of Amasya red apples, Food and Bioproducts Processing 88 (2010) 124–132.
[6] B.M.A. Amer, M.A. Hossain, K. Gottschalk, Design and performance evaluation of a new hybrid solar dryer for banana, Energy Conversion and Management 51 (2010) 813–820.

[7] X. Daun, Z. Min, S.M. Arun, W. Shaojin, Microwave freeze drying of sea cucumber (*Stichopus japonicus*), Journal of Food Engineering 96 (2010) 491–497.
[8] A.O. Dissa, H. Desmoricux, P.W. Savadoge, B.G. Segda, J. Koulidiati, Shrinkage, porosity and density behaviour during convective drying of spirulina, Journal of Food Engineering 97 (2010) 410–418.
[9] A. Kilic, Low temperature and high velocity (LTHV) application in drying: characteristics and effects on the fish quality, Journal of Food Engineering 91 (2009) 173–182.
[10] A. Demirbas, Use of algae as biofuel sources, Energy Conversion and Management 51 (2010) 2738–2749.
[11] S. Amin, Review on biofuel oil and gas production processes from microalgae, Energy Conversion and Management 50 (2009) 1834–1840.
[12] L. Ge, W. Peng, M. Haijin, Study on saccharification techniques of seaweed wastes for the transformation of ethanol, Renewable Energy 36 (2011) 84–89.
[13] A. Vergara-Fernandez, G. Vargas, N. Alarcon, A. Velasco, Evaluation of marine *laminaria japonica* as source of biogas in a two-stage anaerobic reactor system, Biomass and Bioenergy 32 (2007) 338–344.
[14] S. Gupta, S. Cox, N. Abu-Ghannam, Effect of different drying temperatures on the moisture and phytochemical constituents of edible Irish brown seaweed, LWT-Food Science and Technology 44 (2011) 1266–1272.
[15] A. Fudholi, M.Y. Othman, M.H. Ruslan, M. Yahya, A. Zaharim, K. Sopian, The effects of drying air temperature and humidity on drying kinetics of seaweed, in: Recent Research in Geography, Geology, Energy, Environment and Biomedicine, Corfu, Greece, 2011, pp. 129–133.
[16] A. Fudholi, M.Y. Othman, M.H. Ruslan, M. Yahya, A. Zaharim, K. Sopian, Design and testing of solar dryer for drying kinetics of seaweed in Malaysia, in: Recent Research in Geography, Geology, Energy, Environment and Biomedicine, Corfu, Greece, 2011, pp. 119–124.
[17] A. Fudholi, M.H. Ruslan, L.C. Haw, S. Mat, M.Y. Othman, A. Zaharim, K. Sopian, Mathematical modeling of brown seaweed drying curves, in: Proceedings of the WSEAS International Conference on Applied Mathematics in Electrical and Computer Engineering, USA, 2012, pp. 207–211.
[18] A. Akbulut, A. Durmus, Energy and exergy analyses of thin layer drying of mulberry in a forced solar dryer, Energy 35 (2010) 1754–1763.
[19] E.K. Akpinar, Drying of mint leaves in a solar dryer and under open sun: modelling, performance analyses, Energy Conversion and Management 51 (12) (2010) 2407–2418.
[20] S. Meziane, Drying kinetics of olive pomace in a fluidized bed dryer, Energy Conversion and Management 52 (3) (2011) 1644–1649.
[21] A.A. El-Sebaii, S. Aboul-Enein, M.R.I. Ramadan, S.M. Shalaby, B.M. Moharram, Thermal performance investigation of double pass-finned plate solar air heater, Applied Energy 88 (2011) 1727–1739.
[22] D.F. Basri, A. Fudholi, M.H. Ruslan, Drying characteristics of the borneo *Canarium odontophyllum* (dabai) fruit, American Journal of Agricultural and Biological Science 7 (3) (2012) 347–356.
[23] M.Y. Othman, A. Fudholi, K. Sopian, M.H. Ruslan, M. Yahya, Analisis kinetik pengeringan rumpai laut *Gracilaria cangii* menggunakan sistem pengering suria (drying kinetics analysis of seaweed *Gracilaria cangii* using solar drying system), Sains Malaysiana 41 (2) (2012) 245–252.
[24] T.Y. Tunde-Akintunde, Mathematical modeling of sun and solar drying of chilli pepper, Renewable Energy 36 (8) (2011) 2139–2145.
[25] A. Fudholi, M.Y. Othman, M.H. Ruslan, K. Sopian, Drying of Malaysian *Capsicum annuum* L. (red chili) dried by open and solar drying, International Journal of Photoenergy (2013) 1–9.
[26] A. Fudholi, M.H. Ruslan, M.Y. Othman, M.S.M. Azmi, A. Zaharim, K. Sopian, Drying of palm oil fronds in solar dryer with finned double-pass solar collectors, WSEAS Transactions on Heat and Mass Transfer 4 (7) (2012) 105–114.
[27] W. Van Gool, Energy policy: fairly tales and factualities, in: O.D.D. Soares, A. Martins da Cruz, G. Costa Pereira, I.M.R.T. Soares, A.J.P.S. Reis (Eds.), Innovation and Technology – Strategies and Policies, Kluwer Academic Publishers, Dordrecht, 1997, pp. 93–105.
[28] P.M. Azoubel, M.D.A.M. Baima, M.D.R. Amorim, S.S.B. Oliveira, Effect of ultrasound on banana cv Pacovan drying kinetics, Journal of Food Engineering 97 (2) (2010) 194–198.
[29] L.A. Duc, J.W. Han, D.H. Keum, Thin layer drying characteristics of rapeseed (*Brassica napus* L.), Journal of Stored Products Research 47 (1) (2011) 32–38.
[30] I. Doymaz, Drying behaviour of green beans, Journal of Food Engineering 69 (2) (2005) 161–165.
[31] I. Doymaz, Drying characteristics and kinetics of okra, Journal of Food Engineering 69 (3) (2005) 275–279.
[32] S. Simal, A. Femenia, M.C. Garau, C. Rosselló, Use of exponential, Page's and diffusion models to simulate the drying kinetics of kiwi fruit, Journal of Food Engineering 66 (3) (2005) 323–328.
[33] M. Ibrahim, K. Sopian, W.R.W. Daud, Study of the drying kinetics of Lemon grass, The American Journal of Applied Sciences 6 (6) (2009) 1070–1075.
[34] R.L. Earle, Unit Operations in Food Processing, Second ed., Pergamon Press, Oxford, 1983, pp. 189.